JACS
JOURNAL OF THE AMERICAN CHEMICAL SOCIETY

Perspective

pubs.acs.org/JACS

The Li-Ion Rechargeable Battery: A Perspective

John B. Goodenough* and Kyu-Sung Park

Texas Materials Institute and Materials Science and Engineering Program, The University of Texas at Austin, Austin, Texas 78712, United States

ABSTRACT: Each cell of a battery stores electrical energy as chemical energy in two electrodes, a reductant (anode) and an oxidant (cathode), separated by an electrolyte that transfers the ionic component of the chemical reaction inside the cell and forces the electronic component outside the battery. The output on discharge is an external electronic current I at a voltage V for a time Δt. The chemical reaction of a rechargeable battery must be reversible on the application of a charging I and V. Critical parameters of a rechargeable battery are safety, density of energy that can be stored at a specific power input and retrieved at a specific power output, cycle and shelf life, storage efficiency, and cost of fabrication. Conventional ambient-temperature rechargeable batteries have solid electrodes and a liquid electrolyte. The positive electrode (cathode) consists of a host framework into which the mobile (working) cation is inserted reversibly over a finite solid−solution range. The solid−solution range, which is reduced at higher current by the rate of transfer of the working ion across electrode/electrolyte interfaces and within a host, limits the amount of charge per electrode formula unit that can be transferred over the time $\Delta t = \Delta t(I)$. Moreover, the difference between energies of the LUMO and the HOMO of the electrolyte, i.e., electrolyte window, determines the maximum voltage for a long shelf and cycle life. The maximum stable voltage with an aqueous electrolyte is 1.5 V; the Li-ion rechargeable battery uses an organic electrolyte with a larger window, which increase the density of stored energy for a given Δt. Anode or cathode electrochemical potentials outside the electrolyte window can increase V, but they require formation of a passivating surface layer that must be permeable to Li^+ and capable of adapting rapidly to the changing electrode surface area as the electrode changes volume during cycling. A passivating surface layer adds to the impedance of the Li^+ transfer across the electrode/electrolyte interface and lowers the cycle life of a battery cell. Moreover, formation of a passivation layer on the anode robs Li from the cathode irreversibly on an initial charge, further lowering the reversible Δt. These problems plus the cost of quality control of manufacturing plague development of Li-ion rechargeable batteries that can compete with the internal combustion engine for powering electric cars and that can provide the needed low-cost storage of electrical energy generated by renewable wind and/or solar energy. Chemists are contributing to incremental improvements of the conventional strategy by investigating and controlling electrode passivation layers, improving the rate of Li^+ transfer across electrode/electrolyte interfaces, identifying electrolytes with larger windows while retaining a Li^+ conductivity $\sigma_{Li} > 10^{-3}$ S cm^{-1}, synthesizing electrode morphologies that reduce the size of the active particles while pinning them on current collectors of large surface area accessible by the electrolyte, lowering the cost of cell fabrication, designing displacement-reaction anodes of higher capacity that allow a safe, fast charge, and designing alternative cathode hosts. However, new strategies are needed for batteries that go beyond powering hand-held devices, such as using electrode hosts with two-electron redox centers; replacing the cathode hosts by materials that undergo displacement reactions (e.g. sulfur) by liquid cathodes that may contain flow-through redox molecules, or by catalysts for air cathodes; and developing a Li^+ solid electrolyte separator membrane that allows an organic and aqueous liquid electrolyte on the anode and cathode sides, respectively. Opportunities exist for the chemist to bring together oxide and polymer or graphene chemistry in imaginative morphologies.

INTRODUCTION

Modern civilization has become dependent on fossil fuels of finite supply and uneven global distribution, which has two problematic consequences: (1) vulnerability of nation states to fossil-fuel imports and (2) CO_2 emissions that are acidifying our oceans and creating global warming. The Li-ion rechargeable battery (LIB) has enabled the wireless revolution of cell phones, laptop computers, digital cameras, and iPads that has transformed global communication. This technology has raised the following pressing question: Can this or another electrochemical technology enable modern civilization to secure a sustainable, distributed energy supply for all people and reduce the imprint on air pollution of the internal combustion engine and coal-fired power plants? A portable rechargeable battery and the electrochemical capacitor can, together, displace the internal combustion engine by powering electric vehicles, but how safely, at what cost, and over how great a driving range? A stationary rechargeable battery can store efficiently electrical energy generated by solar and/or wind power, and it can provide a distributed or a centralized energy store, but for how long a shelf and cycle life, with how rapid a response to a power outage or fluctuation in the grid, and with how large a capacity at a competitive cost?

A battery is made of one or more interconnected electrochemical cells each giving a current at a voltage for a time Δt. The output current I and/or time Δt to depletion of the stored energy in a battery can be increased by enlarging the area of the electrodes or connecting cells in parallel; the voltage V for a desired power $P = IV$ by connecting cells in series. Here we

Received: September 14, 2012
Published: January 7, 2013

   dx.doi.org/10.1021/ja3091438 | J. Am. Chem. Soc. 2013, 135, 1167−1176

address only issues related to strategies for individual rechargeable battery cells; the management of the individual cells of a battery becomes more complex, as does the cost, the larger the number of cells needed for a given battery application.

ELECTROCHEMICAL CELLS

An electrochemical cell consists of two electrodes, the anode and the cathode, separated by an electrolyte. The electrolyte may be a liquid or a solid. Solid electrolytes are used with gaseous or liquid electrodes; they may be used with solid electrodes, but solid−solid interfaces are problematic unless the solid electrolyte is a polymer or the solid electrodes are thin. Solid electrodes separated by a liquid electrolyte are kept apart by an electrolyte-permeable separator.

The electrolyte conducts the ionic component of the chemical reaction between the anode and the cathode, but it forces the electronic component to traverse an external circuit where it does work, Figure 1. Because the ionic mobility in the electrolyte is

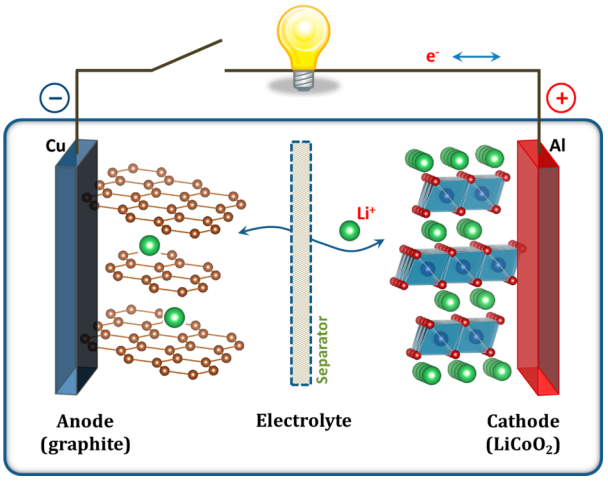

Figure 1. Schematic illustration of the first Li-ion battery ($LiCoO_2$/Li^+ electrolyte/graphite).

much smaller than the electronic conductivity in a metal, a cell has large-area electrodes separated by a thin electrolyte; metallic current collectors deliver electronic current from/to the redox centers of the electrodes to/from posts that connect to the external circuit. A rechargeable cell has a reversible chemical reaction at the two electrodes.

During discharge and charge, an internal battery resistance R_b to the ionic current $I_i = I$ reduces the output voltage V_{dis} from the open-circuit voltage V_{oc} by a polarization $\eta = I_{dis}R_b$ and increases the voltage V_{ch} required to reverse the chemical reaction on charge by an overvoltage $\eta = I_{ch}R_b$:

$$V_{dis} = V_{oc} - \eta(q, I_{dis}) \tag{1.1}$$

$$V_{ch} = V_{oc} + \eta(q, I_{ch}) \tag{1.2}$$

where q represents the state of charge. The percent efficiency of a cell to store energy at a fixed current I is

$$100 \times \frac{\int_0^{Q_{dis}} V_{dis}(q)\mathrm{d}q}{\int_0^{Q_{ch}} V_{ch}(q)\mathrm{d}q} \tag{2}$$

$$Q = \int_0^{\Delta t} I\mathrm{d}t = \int_0^{Q} \mathrm{d}q \tag{3}$$

where Q is the total charge per unit weight (Ah kg^{-1}) or per volume (Ah L^{-1}) transferred by the current $I = dq/dt$ on discharge or charge. $Q(I)$ is referred to as the cell capacity for a given I; Q depends on I because the rate of transfer of ions across electrode/electrolyte interfaces becomes diffusion-limited at high currents. A diffusion-limited loss of the Li inserted into an electrode particle at a high rate of charge or discharge represents a reversible loss of capacity. However, on charge/discharge cycling, changes in electrode volume, electrode−electrolyte chemical reactions, and/or electrode decomposition can cause an irreversible loss of capacity. Electrode−electrolyte chemical reactions that result in the irreversible formation of a passivating solid−electrolyte interphase (SEI) layer on an electrode during an initial charge of a cell fabricated in a discharged state are distinguished from the irreversible capacity fade that may occur with cycling. The percent Coulombic efficiency of a single cycle associated with a capacity fade is

$$100 \times \frac{Q_{dis}}{Q_{ch}} \tag{4}$$

The cycle life of a battery is the number of cycles until the capacity fades to 80% of its initial reversible value. Additional figures of merit of a rechargeable cell, aside from cost and safety, are its density (specific and volumetric) of stored energy, its output power $P(q) = V(q)I_{dis}$ for a given discharge current, and its calendar (shelf) life. The available energy stored in a fully charged cell depends on the discharge current I_{dis}; it may be obtained by measuring the time $\Delta t(I_{dis})$ for its complete discharge at a constant $I_{dis} = dq/dt$:

$$\text{energy} = \int_0^{\Delta t} IV(t)\mathrm{d}t = \int_0^{Q} V(q)\mathrm{d}q \tag{5}$$

The gravimetric energy density (Wh kg^{-1} or mWh g^{-1}) is dependent on I_{dis} through $Q(I_{dis})$. The volumetric energy density (Wh L^{-1}) is of particular interest for portable batteries, especially those that power hand-held or laptop devices. The tap density is a measure of the volume fraction of active particles in a cylinder after "tapping", i.e., of the packing density of active electrode particles.

THE CHALLENGE

The LIB has created great changes in modern life. We have been using cell phones to communicate with others and laptop computers to work anywhere. Moreover, the recent developments of smart phones and tablet computers have provided more user experience, but these developments continue to request more operating cycles in electronic devices with thinner and lighter LIBs of higher stored energy. Yoshino[1] of the Asahi Kasei Corporation assembled the first $Li_{1-x}CoO_2$/C cell (Figure 1), which was commercialized by the SONY Corporation in a cell phone and a camcorder. The energy stored in a hand-held LIB has since been successfully increased to >3.0 Ah in the 18 650 cell now available. However, the volumetric energy density has been increased mainly by cell engineering; and sophisticated cell engineering, including the ability of the synthetic chemist to control the size and morphology of the active particles as well as the architecture of the current collectors, has almost reached its limits. Realization of affordable electric vehicles competitive with cars powered by the internal combustion engine and storage of electrical energy generated by solar and/or wind power will require new battery strategies.

dx.doi.org/10.1021/ja3091438 | J. Am. Chem. Soc. 2013, 135, 1167−1176

The present-day LIB is fabricated in a discharged state. It uses reversible Li extraction from an oxide host as the rechargeable cathode and into carbon or buffered spongy silicon or tin as the anode host. The capacity of an oxide host is limited to the reversible solid−solution range of Li in the cathode host structure operating on the redox energy of a single transition-metal cation; and where a passivating layer forms on the anode during the first charge, the capacity is further reduced by an irreversible loss of Li from the cathode in the Li^+-permeable SEI layer formed on the anode. Nevertheless, rechargeable batteries capable of over 30 000 safe charge/discharge cycles at an acceptable rate, equivalent to a 10 year operational life, have been achieved.[2] Therefore, the essential challenge for the chemist and electrochemical engineer is to develop a strategy that will retain this cycle life at an acceptable rate in a safe, affordable battery with a much larger energy density than is realizable with present strategies.

From eq 5, the stored energy is the product of the average voltage $<V(q)>$ and the capacity $Q(I)$. The open-circuit voltage of a cell is the difference between the electrochemical potentials μ_A and μ_C of the anode and cathode:

$$V_{OC} = (\mu_A - \mu_C)/e \quad (6)$$

This voltage is limited by either the "window" of the electrolyte or the top of the anion-p bands of the cathode. The window of the electrolyte, illustrated in Figure 2a,b, is the energy gap between its lowest unoccupied and highest occupied molecular orbitals (LUMO and HOMO) of a liquid electrolyte or the bottom of the conduction band and top of the valence band of a solid electrolyte. As illustrated in Figure 2a,b, a μ_A above the electrolyte LUMO reduces the electrolyte unless the anode−electrolyte reaction becomes blocked by the formation of a passivating SEI layer; similarly, a μ_C located below the HOMO oxidizes the electrolyte unless the reaction is blocked by an SEI layer. However, μ_C cannot be lowered below the top of the cathode anion-p bands, which may have an energy above the electrolyte HOMO. The top of the sulfide S-3p bands of the layered sulfides $LiMS_2$ is ~2.5 eV below the μ_A of a Li anode, $\mu_A(Li)$, whereas the top of the O-2p bands of the layered oxides $LiMO_2$ is ~4.0 eV below $\mu_A(Li)$, which is why oxide hosts are used as cathodes of present day LIBs.[3,4] Since the practical HOMO of the organic liquid carbonate electrolytes used in LIBs is at 4.3 eV below $\mu_A(Li)$, the voltage of the simple $LiMO_2$ layered oxides is also self-limited by the energy of the top of the O-2p bands, Figure 2c. As a result, the original $Li_{1-x}CoO_2$ cathode evolves oxygen or inserts protons on removing Li^+ beyond $x = 0.55$.[5]

To understand this phenomenon, consider a transition-metal redox energy near the top of the anion-p bands. On oxidation of the couple, the empty states experience a strong anion-p/M-d covalent admixture. In $Li_{1-x}CoO_2$, for example, the Co(IV)/Co(III) couple is near the top of the O-2p bands, and the holes introduced into the Co(IV)/Co(III) couple by removal of Li^+ are initially in Co(IV) polaronic states, but in the interval $0.5 < x < 0.9$, there is a crossover from polaronic to itinerant holes in states of d-orbital symmetry. This crossover is first-order, which means that a phase segregation into Li-poor and Li-rich regions occurs to give a constant $V(q)$. However, at $x > 0.55$, the added itinerant holes become trapped in O-2p molecular orbitals of peroxide $(O_2)^{2-}$ ions at the particle surface, which is followed by O_2 evolution. Not only is μ_C pinned at the top of the O-2p bands, it also becomes impossible to oxidize the Co beyond a Co(IV)/Co ratio of 0.55.

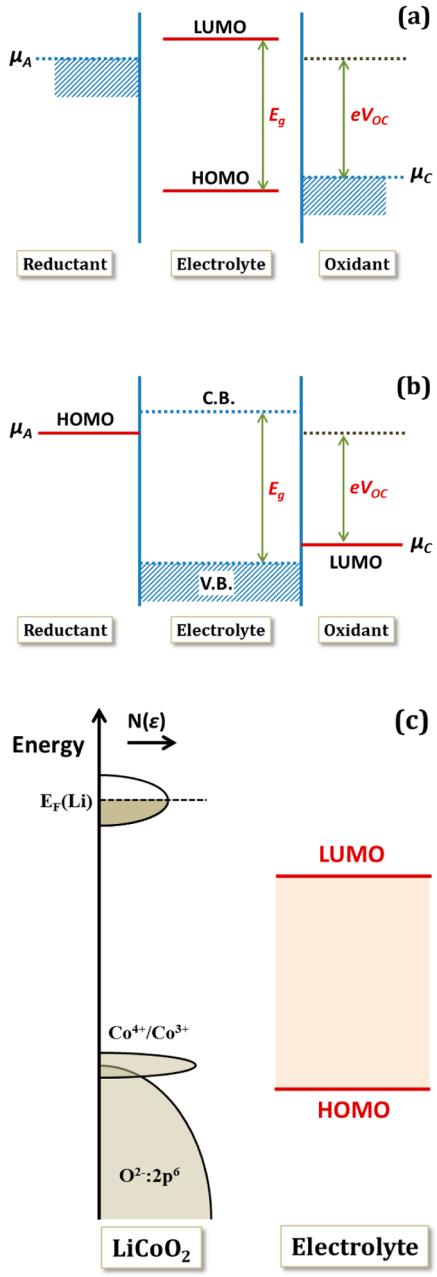

Figure 2. Relative energies of the electrolyte window E_g and the electrode electrochemical potentials μ_A and μ_C with no electrode/electrolyte reaction: (a) liquid electrolyte with solid electrodes; (b) solid electrolyte with liquid or gaseous reactants. (c) Schematic energy diagram of $\mu_A(Li)$ and $\mu_A(LiCoO_2)$ and their relative energy positions with respect to the HOMO and LUMO of a carbonate-based electrolyte.

Although the top of the O-2p bands of an oxide host can be lowered to more than 5 eV below $\mu_A(Li)$ by replacing an oxide ion with a polyanion as in $LiNiPO_4$, investigation of these high-voltage cathodes has been limited because the organic liquid carbonate electrolytes used in the LIBs decompose at a voltage $V > 5$ V. Moreover, the counter cation used to lower the top of the O-2p bands reduces the capacity unless the active redox center can accommodate two electrons without a voltage step between them, e.g., a Ni(II) to Ni(IV) reaction in the spinel $Li[Ni_{0.5}Mn_{1.5}]O_4$, where pinning of the $\mu_C(Ni)$ at the top of the O-2p bands creates itinerant electrons in states of d-orbital symmetry. Increasing the host cathode voltage without sacrifice of capacity is under intensive

dx.doi.org/10.1021/ja3091438 | J. Am. Chem. Soc. 2013, 135, 1167−1176

investigation for the plug-in hybrid electric vehicle, which is an intermediate-term solution for partial displacement of the internal combustion engine.

With a cathode voltage limited to $V \lesssim 5$ V vs Li, an increase in stored energy density for powering an all-electric vehicle requires a large increase in the cathode capacity over what can be obtained with a Li-insertion host. For this application, attention has turned to the use of inexpensive multielectron redox centers, e.g., elemental double-bonded reactants sulfur and gaseous O_2. On the other hand, the primary driver for a stationary battery is not energy density, but total energy stored at a competitive cost. Moreover, stationary batteries do not need to operate in the low temperatures encountered by an automobile in a Canadian winter. Therefore, for stationary storage of electrical energy, attention has turned to the development of electrochemical cells with solid membranes that allow use of flow-through couples in liquid cathodes.

RECHARGEABLE LI-ION BATTERIES: THEIR EVOLUTION

A rechargeable battery must have reversible chemical reactions at both electrodes. Reversible chemical reactions at solid electrodes are of two types: displacement and insertion reactions. Solid cathodes undergo insertion reactions, and solid anodes commonly undergo displacement reactions, but insertion reactions are also used. A rechargeable battery may be assembled in either the charged or discharged state; primary (nonrechargeable) batteries can only be fabricated in a charged state.

Electrodes undergoing insertion reactions consist of an electronically conducting host structure into/from which the working cation, e.g., H^+ or Li^+, can be inserted/extracted reversibly over a finite solid−solution range; e.g., the cathode reaction:

$$x\mathrm{H}^+ + x\mathrm{e}^- + \mathrm{NiOOH} = \mathrm{NiO}_{1-x}(\mathrm{OH})_{1+x} \tag{7}$$

with $0 < x < 1$ that has the energy of the Ni(III)/Ni(II) redox couple well-matched to the O_2/H_2O HOMO of an alkaline aqueous electrolyte. The anode of an aqueous-electrolyte battery may be either an insertion host, e.g., a metal hydride MH_x, or an elemental metal that undergoes a displacement reaction, e.g.:

$$\mathrm{Cd} + 2x\mathrm{H_2O} - 2x\mathrm{e}^- = \mathrm{Cd(OH)_2} + 2x\mathrm{H}^+ \tag{8}$$

Cadmium has an electrochemical potential $\mu_A(\mathrm{Cd})$ well-matched to the H_2/H_2O LUMO of an alkaline electrolyte. The (NiOOH)/Cd cell is assembled in a charged state[6] and gives a $V \simeq 1.5$ V.

The window of an aqueous electrolyte restricts the voltage of a battery with a stable shelf life to $V \leq 1.5$ V. The Li-ion battery was motivated by the need for a rechargeable battery with a larger energy density, i.e., a larger voltage, which requires a nonaqueous electrolyte. Since H^+ is only mobile in an aqueous medium, Li^+ was chosen as the working ion in a nonaqueous electrolyte. Li salts are soluble and separable in ethers or in the organic dimethyl and diethyl liquid carbonates (DMC and DEC).[7] These electrolytes offer a window of ~3 eV, but the carbonates offer a lower practical HOMO at ~4.3 eV below $\mu_A(\mathrm{Li})$,[8] and primary (unrechargeable) Li batteries with these electrolytes were known to support the anode displacement reaction:

$$\mathrm{Li} = \mathrm{Li}_{1-x} + x\mathrm{Li}^+ + x\mathrm{e}^- \tag{9}$$

provided the electrolyte included an ethylene carbonate (EC) additive to passivate the Li anode.[9] The $\mu_A(\mathrm{Li})$ is ~1.1 eV above the LUMO of the DMC/DEC electrolytes.[10] Like most innovative technologies, the genesis of the LIB came from fundamental studies. In 1970, Jean Rouxel of France and Robert Schöllhorn of Germany were exploring the chemistry of reversible Li intercalation into layered transition-metal sulfides and selenides. Physicists were interested in this chemistry as metallic mixed-valent electronic conductivity in the 2D layers exhibited charge-density waves, and TiS_2 appeared to represent a 2D superconductor. Since a reversible chemical reaction is needed for a rechargeable cathode, Brian Steele[11] suggested that TiS_2 could offer a cathode for a rechargeable LIB, and in 1976, Whittingham[12] demonstrated a fast rechargeable TiS_2/Li cell with a $\langle V \rangle \simeq 2.2$ V. The first energy crisis of the early 1970s had activated a wider interest in energy technologies, and the Whittingham demonstration immediately triggered efforts to commercialize a LIB assembled in the charged state with a layered-sulfide cathode. Unfortunately, although the SEI layer that forms with EC to passivate the Li anode is permeable to Li^+, it prevents uniform plating of Li during charge in a rechargeable cell.[13] Consequently, dendrites form and, on repeated charging, can grow across the separator to give an internal short-circuit with incendiary, even explosive, consequences.[14] As a result, the initial efforts to commercialize a LIB were abruptly abandoned. Nevertheless, lithium can be the anode not only in a primary Li battery but also in a "half-cell" used to evaluate the voltage and performance of a cathode; but it cannot be used safely as the anode of a rechargeable cell with an organic electrolyte.

However, the concept of a LIB was not abandoned. Goodenough recognized that increasing the voltage of the anode would require a cathode providing a larger voltage vs Li. He also noted that the voltage attainable with a layered sulfide would be limited to ~2.5 V vs Li since the bottom of the Ti(IV)/Ti(III) conduction band of TiS_2 is only 0.2 eV above the top of the S-3p bands. The oxides would offer O-2p bands at a lower energy, and his early experience[15] with $Li_xNi_{1-x}O$ with $0 \leq x \leq 0.5$ led him to explore with his group at Oxford the extraction of Li from the layered oxides $LiMO_2$ with M = Cr, Co, Ni. The disproportionation reaction 3Cr(IV) = 2Cr(III) + Cr(VI) with the Cr(VI) occupying interlayer tetrahedral sites eliminated $LiCrO_2$, but the group showed that $LiCoO_2$ and $LiNiO_2$ give a reversible Li extraction at a $V \simeq 4.0$ V vs Li. Since the battery community was accustomed to fabricating charged batteries, it remained largely unimpressed by the fabrication of a discharged cathode. Meanwhile, Rachid Yazami was exploring Li intercalation into graphite and noted that reversible Li insertion into carbon avoids the problem of dendrite formation,[16] but a $\mu_A(\mathrm{Li}) - \mu_A(\mathrm{C}) \approx 0.2$ eV prevents a fast charge that raises V_{ch} of eq 1.2 to where Li is plated on the surface of the carbon more rapidly than Li^+ is inserted into the carbon.[17] Although a carbon anode restricts the rate of charge, the first Li-ion battery, Figure 1, was assembled by Yoshino[1] with a discharged carbon anode and a discharged $LiCoO_2$:

$$\mathrm{C} + x\mathrm{e}^- + x\mathrm{Li}^+ = \mathrm{Li}_x\mathrm{C(anode)} \tag{10.1}$$

$$\mathrm{LiCoO_2} - x\mathrm{e}^- - x\mathrm{Li}^+ = \mathrm{Li}_{1-x}\mathrm{CoO_2(cathode)} \tag{10.2}$$

Insertion of a guest Li^+ into a layered host like TiS_2, CoO_2, or graphite was originally referred to as intercalation.[18]

Fabrication of $LiMO_2$ with Li^+ and M(III) well-ordered into alternate (111) octahedral-site planes of the cubic-close-packed oxide-ion array requires a Li^+ ionic radius larger than the M(III)-ion radius,[19] which is why it is easier to obtain better ordering of $NaMO_2$ than of $LiMO_2$ compounds and why low-spin Co(III): t^6e^0 is better ordered than low-spin Ni(III): t^6e^1. However, the Co(IV)/Co(III) and Ni(IV)/Ni(III) couples are both pinned at

dx.doi.org/10.1021/ja3091438 | J. Am. Chem. Soc. 2013, 135, 1167−1176

the top of the O-2p bands, so $Li_{1-x}CoO_2$ evolves O_2 for $x > 0.55$ and $Li_{1-x}NiO_2$ for $x > 0.8$. To reduce material cost and extend capacity, the $LiNi_{1-x}Co_xO_2$ oxides were investigated.[20] Nevertheless, O_2 evolution inside a cell creates safety problems unless the cell voltage is carefully managed. The addition of ~10% Al^{3+} stabilizes the layered oxides against electrode/electrolyte interface reactions on Li extraction, but at the expense of capacity.[21] Another safety issue is internal short-circuits by Li penetration across the separator or by direct cathode and anode contact through a pinhole or thermal shrinkage. To eliminate this problem, a slurry of Al_2O_3 and a polymeric binder is coated on the separator to block Li-dendrite penetration.

Li-ion rechargeable batteries are more easily fabricated in their discharged state. During charge, Li ions from the cathode are inserted into a discharged anode. However, if the Fermi energy μ_A of the charged anode is above the LUMO of the electrolyte, which is the case with a carbon anode at 0.2 V vs Li, a fraction of the Li from the cathode is consumed irreversibly on the initial charge in the passivating Li^+-permeable SEI layer that forms on the anode surfaces. Moreover, the SEI layer increases the impedance of Li^+ transfer across the anode/electrolyte interface, and the SEI layer changes with successive cycling to contribute to a capacity fade.

Since carbon has a limited capacity (Li_xC with $0 \le x \le 1/6$ in graphite) and Li is plated onto its surface in a fast charge, the carbon anode is being replaced by insertion into Si or alloys of Sn or Sb. These Li alloys have a μ_A 0.2−0.8 eV below μ_A(Li), which allows a fast charge without Li plating, and they have a much larger capacity than carbon. However, a huge lattice expansion (~300% for Si) on Li insertion requires that the active anode be assembled as small particles or a sponge-like array within a Li^+ and electron conductive medium that is sufficiently elastic to absorb the volume changes. Moreover, a $\mu_A \le 0.2$ V vs Li does not allow safe fast charge that is desired for an electric vehicle battery. The buffering medium may be carbon or a conductive polymer. However, a $\mu_A(Li) - \mu_A(alloy) < 1.1$ eV still requires formation of an SEI layer with the organic liquid-carbonate electrolyte, which robs Li irreversibly from the cathode on the initial charge and introduces a variable impedance to Li^+ transport across the anode/electrolyte interface. In an attempt to improve the stability and lower the impedance of the SEI layer, replacement of EC by other additives to the electrolyte, e.g. fluoroethylene carbonate,[22] is being explored.

In 1967, Kummer and Weber[23] had discovered fast 2D Na^+ transport in $Na_2O{\cdot}11Al_2O_3$, which offered the possibility of a rechargeable battery with molten electrodes and a solid electrolyte. One result of this discovery was an attempt to develop Na^+ and Li^+ electrolytes exhibiting fast 3D alkali-ion transport. Out of this endeavor came the concept of framework hosts[24] (originally referred to as skeleton structures) for fast 3D alkali-ion transport. The larger Na^+ ion requires a relatively large 3D interstitial space as exemplified by $Na_3Zr_2PSi_2O_{12}$ having the hexagonal $Fe_2(SO_4)_3$ framework of Figure 3. This Na^+ electrolyte was later referred to as NASCICON for NA SuperIonic CONductor. The Li^+ ion, on the other hand, is small enough to be mobile at room temperature in a close-packed oxide-ion array, as exemplified by the layered oxides $LiMO_2$. However, these 2D Li^+ conductors have a degree of freedom along the c axis. The $A[B_2]O_4$ spinel structure of Figure 4 also has a cubic close-packed oxide-ion array, but it is strongly bonded in 3D. Nevertheless, the $[B_2]O_4$ framework provides fast Li^+ transport in 3D. An investigation[25] of Li insertion into the spinel Fe_3O_4 led to the realization that the Li^+ were pushing all the tetrahedral-site Fe(III) in a cascade into the empty 16c octahedral sites to transform the spinel

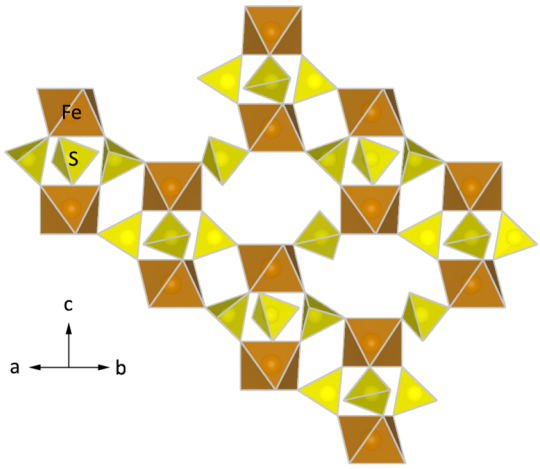

Figure 3. Hexagonal $Fe_2(SO_4)_3$ framework having 3D interconnected lantern units.

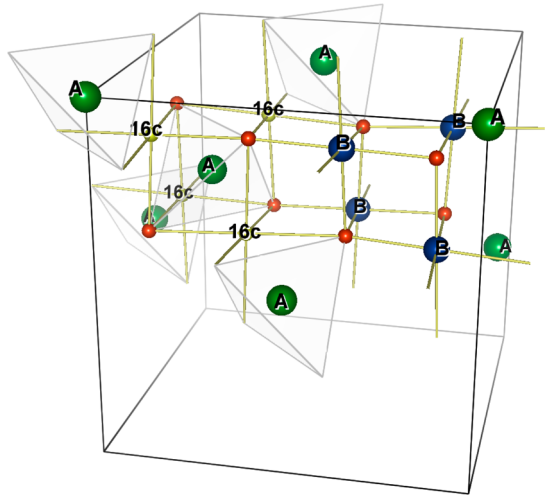

Figure 4. (a) Two quadrants of an $A[B_2]O_4$ spinel structure showing octahedral 16c sites bridging tetrahedral 8a sites (A atoms).

phase to a rock-salt phase containing the spinel $[B_2]O_4$ framework intact. This experiment showed the $[B_2]O_4$ array of the spinel structure provides a strongly bonded framework in which Li^+ are mobile at room temperature in a 3D interstitial space consisting of the tetrahedral A sites bridged by the 16c octahedral sites sharing faces with two A sites on opposite sides. This realization led immediately to an investigation of $Li[Mn_2]O_4$ as a LIB cathode.[26,27]

Comparison of the Li^+ sites in the layered Li_xMnO_2 and $Li_{2x}[Mn_2]O_4$ oxides is instructive. Whereas the Li^+ would occupy only octahedral sites for all $0 < x < 1$ compositions in Li_xMO_2, the $Li_{2x}[Mn_2]O_4$ oxides contain Li^+ in all tetrahedral A sites with $0 < x < 0.5$ and in all octahedral 16c sites with $0.5 < x < 1$. Moreover, the tetrahedral A sites form a diamond array consisting of two interpenetrating face-centered cubic arrays, which stabilizes an ordered phase at $x = 0.25$ in which Li^+ occupy only one of these A-site arrays. The energy of an M(IV)/M(III) redox couple shows a surprising sensitivity to the Li^+ order on tetrahedral sites by exhibiting two plateaus at $0 < x < 0.25$ and $0.25 < x < 0.5$ near 4 V vs Li with a small voltage step between them and an abrupt drop from 4 to 3 V at $x = 0.5$ where the Li^+ shift from tetrahedral to octahedral sites (Figure 5). This sensitivity limits use of the spinel framework as a cathode material to only a single Li^+ per two framework cations, whereas the layered compounds would,

dx.doi.org/10.1021/ja3091438 | J. Am. Chem. Soc. 2013, 135, 1167−1176

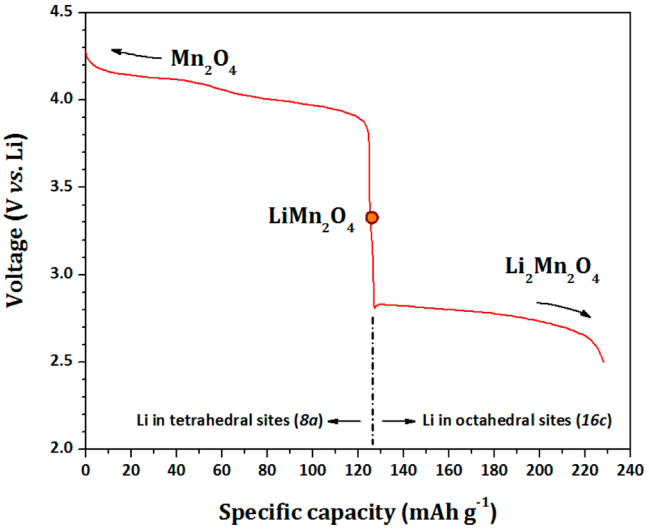

Figure 5. Voltage curves for Li^+ insertion and extraction of $LiMn_2O_4$.

theoretically, offer a Li^+ for every layered M cation (as in Li_xTiS_2) if there were no pinning of the redox couple at the top of the O-2p bands. Nevertheless, in the oxospinels the top of the O-2p bands is lowered sufficiently from 4 eV below $\mu_A(Li)$ in the $LiMO_2$ oxides to access a $<V(q)> \approx 4$ V for $0 < x < 0.5$ without any safety problem associated with O_2 evolution. However, the top of the O-2p bands is also lowered sufficiently that the mixed-valent Mn(IV)/Mn(III) electronic conductivity is polaronic: localized Mn(III):t^3e^1 configurations move diffusively. The e-orbital degeneracy on a localized Mn(III):t^3e^1 high-spin configuration in sufficient concentration gives rise to a cooperative orbital ordering to lower the Mn(III) site symmetry above room temperature.[28] This phenomenon is referred to as a cooperative Jahn−Teller (J-T) distortion after the early recognition of orbital ordering in molecules.[29] In the $Li_{2x}[Mn_2]O_4$ spinels, the concentration of Mn(III) is just high enough at $x = 0.5$ for a cooperative J-T distortion to set in at room temperature. It is responsible for the two-phase plateau in Figure 5 in the interval $0.5 < x < 0.8$ where there is a coexistence of cubic and tetragonal phases. At the surface of the $Li_{2x}[Mn_2]O_4$ particles with $0 < x < 0.5$, ordering of Li^+ at $x = 0.25$ gives a high enough concentration of Mn(III) at the surface on discharge for the disproportionation reaction 2Mn(III) = Mn(II) + Mn(IV), which leads to a dissolution of Mn(II) into the electrolyte where, on cycling, the Mn(II) move to the anode SEI layer to poison the anode reactions. Introducing Ni into the framework substitutes Ni(II) + Mn(IV) for two Mn(III) and lowers the stabilization of Li^+ order at $x = 0.25$, which eliminates the voltage step at $x = 0.25$ and lowers the Mn(III) concentration sufficiently to eliminate problems with cooperative Mn(III)-site distortions in the range $0 < x < 0.5$, but it does not completely eliminate capacity fade on cycling.

These observations have led to investigation of layered $Li(Ni_{1/3+x}Co_{1/3-2x}Mn_{1/3+x})O_2$[30] and $Li(Ni_{0.5}Mn_{0.5})O_2{\cdot}Li_2MnO_3$[31,32] and spinel $Li[Ni_{0.5}Mn_{1.5}]O_4$[33] in which a Mn(IV) and a Ni(II) replace two Mn(III). The Mn(V)/Mn(IV) couple is inaccessible, lying below the top of the O-2p bands, but both the Ni(III)/Ni(II) and the Ni(IV)/Ni(III) couples are accessible. The top of the O-2p bands is lowered to 4.8 eV below $\mu_A(Li)$ and the Ni(III)/Ni(II) and Ni(IV)/Ni(III) to ~4.75 eV below $\mu_A(Li)$. The Ni couples remain close enough to the top of the O-2p bands that the holes introduced into the σ-bonding 3d orbitals of Ni(II) occupy itinerant states of d-orbital symmetry, which eliminates the voltage step between the low-spin Ni(III)/Ni(II) and Ni(IV)/Ni(III) couples.

In the spinel $Li_{1-x}[Ni_{0.5}Mn_{1.5}]O_4$, access to a multielectron redox couple on Ni still provides one mobile Li^+ guest for two framework cations. However, on reacting the spinel above 700 °C, e.g. 900 °C, loss of oxygen is accommodated by the introduction of interstitial cations in a cation-deficient rock-salt second phase and reduction of Mn(IV) to Mn(III). The loss of oxygen and the spinel to rock-salt phase transition are both reversible on cooling in air to below 700 °C, but ordering of the Ni(II) and Mn(IV) in the spinel framework at 700 °C gives too poor an electronic conductivity for a good electrode.[34] Moreover, a $V \simeq 4.75$ V is above the HOMO of the liquid-carbonate electrolytes at 4.0−4.3 V vs Li, which requires formation of a cathode SEI layer to stabilize the spinel. Volume changes on cycling make coating the spinel particles with a Li^+-permeable SEI layer[34] less effective than developing an intrinsic SEI layer by doping with trivalent ions,[35,36] e.g., Fe^{3+} or Cr^{3+}, for a Ni(II) and a Mn(IV). These dopants lower the concentration of Ni on the surface, which stabilizes the particles against capacity fade even at 55 °C, but these dopants leave a residual Mn(III) content that is not removed by an anneal in air at 600 °C. The fabrication of $Li[Ni_{0.5}Mn_{1.5}]O_4$ with excess Mn and cooling from 900 °C at a rate that is slow enough to convert the rock-salt phase back to spinel, but fast enough to prevent long-range ordering of the Ni(II) and Mn(IV), results in a stable cubic spinel with only short-range order of Ni(II) and Mn(IV). Although this spinel offers a high-voltage cathode (Figure 6), the capacity remains

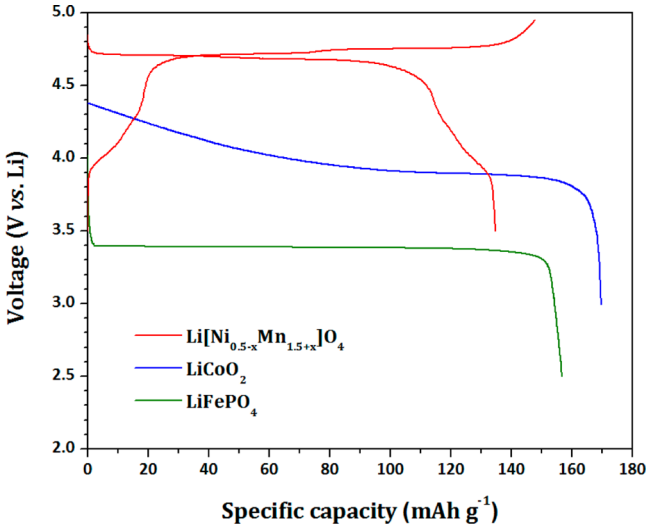

Figure 6. Comparison of charge/discharge voltage curves of $Li[Ni_{0.5-x}Mn_{1.5+x}]O_4$ with those of $LiCoO_2$ and $LiFePO_4$.

below 130 mAh g^{-1}, especially if it loses Li to an anode SEI layer on the initial charge.

On the other hand, the spinel $Li[Li_{1/3}Ti_{5/3}]O_4$ has a Ti(IV)/Ti(III) couple below the LUMO of the liquid-carbonate electrolytes. Li insertion into this spinel at 1.5 V vs Li is without formation of an SEI layer, and it shows little capacity fade after 30 000 charge/discharge cycles at 5C rate.[2] This demonstration shows not only high Li^+ mobility in the close-packed oxide-ion array of the spinel framework, but also that elimination of the anode SEI layer improves greatly the cycle life of the electrode. However, this excellent performance is at a cost of 1.3 V vs a carbon anode or 0.7−1.0 V vs an alloy anode, and the capacity is limited to

dx.doi.org/10.1021/ja3091438 | J. Am. Chem. Soc. 2013, 135, 1167−1176

under 150 mAh g^{-1} to give a poor energy density $<V_{dis}>Q$. Use of this anode for a stationary storage battery will depend on its fabrication cost.

To increase the energy density of a rechargeable battery with solid electrodes to where it can compete with the internal combustion engine, it will be necessary to find a way to raise $<V(q)>$ while retaining a large cathode Q at high currents I. The layered oxides $LiCoO_2$ and $LiNiO_2$ have an intrinsic voltage limit imposed by the top of the O-2p bands at ~4.0 eV below μ_A(Li). On the other hand, the energy of the top of the O-2p bands can be lowered by the introduction of a strongly covalent countercation either by substituting for O^{2-} a polyanion $(XO_4)^{m-}$ with X = Si, P, or S or by replacing some active cations with a cation like Mn(IV) that forms strong bonds with oxygen as in the spinel $Li[Ni_{0.5}Mn_{1.5}]O_4$, for example. In addition to lowering the top of the O-2p bands, these substitutions also lower the energies of antibonding d-electron redox couples through the inductive effect.[37] The $M_2(XO_4)_3$ framework having the hexagonal $Fe_2(SO_4)_3$ structure of Figure 3 is able to host up to five guest Li^+ or four guest Na^+ in its 3D interconnected interstitial space. Although this framework has been used[38] to measure the relative energies of the redox couples of the 3d M cations and their dependence on the X atom of the polyanion, competitive cost and energy densities have not been obtained with this framework host. On the other hand, the $LiMPO_4$ ordered olivines having only a 1D Li motion, Figure 7, have provided $LiFePO_4$ with a V = 3.5 V vs Li.[39] If

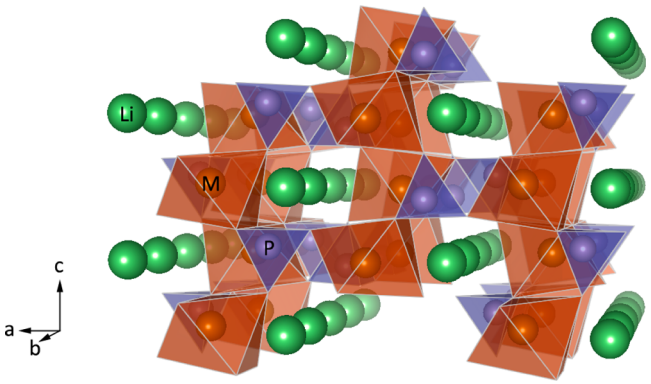

Figure 7. Crystal structure of the olivine $LiMPO_4$.

prepared as nanoparticle platelets having the 1D channels perpendicular to the platelets, this cathode material is safe and has been cycled at a 5C rate for over 30 000 cycles with a large fraction of its theoretical capacity of 170 mAh g^{-1}.[2] The $FePO_4$ framework is inexpensive and environmentally friendly, but the cost of quality control of the $LiFePO_4$ electrodes is presently too high.

$LiFePO_4$ illustrates use of the inductive effect associated with a countercation, in this case P(V), to tune the energy of the active redox couple, in this case the Fe(III)/Fe(II) couple. However, at the surface under-coordination of the Fe and/or longer P−O bonds raises the energy of the Fe(III)/Fe(II) couples near the surface. Raising the energy of the redox couple introduces an added activation energy for Li^+ transport across the electrode/electrolyte interface. In the case of $LiFePO_4$, exposing the surface to S or N anions has been shown[40] to lower the surface charge-transfer impedance, thereby increasing the capacity at higher rates of charge/discharge. These effects on other active particles remain unexplored.

$LiFePO_4$ has also directed attention to the electronic conductivity of a cathode host. Where the active redox couple of the host is near the top of the O-2p bands, holes introduced by oxidation have sufficient O-2p character to be itinerant with a high mobility. Where the energy of the active redox couple is sufficiently far above that of the top of O-2p bands, as is the case in $LiFePO_4$, electronic conductivity is diffusive by small-polaron hopping on a mixed-valent array. A two-phase reaction between $LiFePO_4$ and $FePO_4$ gives a flat output voltage, but it prevents sufficient mixed valence on the iron in either phase to give an adequate polaronic conductivity. Poor electronic conductivity limits the rate of charge and discharge. Therefore, it has proved necessary to either coat small particles of shorter charge-carrier path length with an electronically conductive surface layer and/or reduce the particle size to the nanoscale where a larger range of single-phase reaction occurs.

Sophisticated nanoscience engineering makes it possible to control the particle size and shape, but coated nanoparticles can decrease the tap density and, therefore, the volumetric energy density to where it is no longer sufficient for a portable battery. Moreover, a uniform conductive coat is critical. In the case of $LiFePO_4$, carbon can uniformly coat $LiFePO_4$ particles and, at the same time, block particle sintering and growth under high-temperature heat treatment.[2] However, as the particle size of an active material approaches that of a carbon coat and surrounding carbon-black additives, uniform coverage of the active material becomes more difficult, and a nonuniform dispersion of nanoscale particles may result. Nanoparticles of $LiFePO_4$ have been uniformly coated by a thin layer of conductive polymer.[41]

Ideally, the redox energy of a coated nanosized particle is within the electrolyte window, as is the case of $LiFePO_4$. However, nanosized anode materials like Si or alloys of Sn or Sb have redox energies well-above the LUMO of a liquid Li^+ organic-carbonate electrolyte. Batteries with these anodes, or with a carbon anode, typically show a large irreversible loss of cathode capacity on the initial charge as a result of formation of a Li^+-permeable SEI layer on the anode. Smaller anode particles have a large surface/volume ratio, which decreases the cathode reversible capacity and can cause a problem of overdischarge of a Cu current collector. However, carbon buffering of Sn or Sb alloys allows use of Al current collectors since alloying of Li and Al can be avoided.

It should also be noted that where a host has poor electronic conductivity, chemical attachment of nanoparticles to a conductive carbon current collector, e.g., a carbon foam or particles sandwiched between graphene sheets, can provide the needed electronic conductivity without the need to add a conductive coat. These architectures can eliminate the need to add a significant amount, or any, inactive carbon black and binder to the electrode. Tap densities with these strategies remain to be explored.

In summary, a LIB using solid rechargeable electrodes is capable of a long cycle life at acceptable rates of charge/discharge, but the energy density of individual cells, even with a 4 V cell, makes difficult the manufacture of a cost-competitive battery of sufficient energy density to displace the internal combustion engine of an automobile with long driving range between rapid and convenient liquid-fuel refills. A first step will be plug-in hybrids used for daily commuting. This interim solution would offer a distributed store of electrical energy that can spread the cost of storing off-peak power in a rechargeable battery. Stationary storage of electrical energy from alternative energy sources (wind, solar, nuclear) calls for larger capacities than can be realized with an oxide-host cathode, but the energy density requirement of a mobile battery is relaxed. However, cost is a

dx.doi.org/10.1021/ja3091438 | J. Am. Chem. Soc. 2013, 135, 1167−1176

constraint that has made difficult even replacement of lead-acid batteries with the 2 V $Li[Li_{1/3}Ti_{5/3}]O_4/LiFePO_4$ cell. These challenges are calling for consideration of alternative strategies for storage of electrical energy in an electrochemical cell.

STRATEGIES WITH SOLID ELECTROLYTES

After their discovery of fast 2D Na^+ transport in $Na_2O{\cdot}11Al_2O_3$ (Na ß-Al_2O_3), Kummer and Weber[23] proposed in 1967 the sodium−sulfur battery, which uses cells containing a solid electrolyte separating a molten Na anode and a cathode of molten sulfur impregnated by carbon felt; the battery operates at 300−350 °C. This proposal was quickly modified in South Africa[42] to fabrication of a discharged zebra cell that replaces the sulfur cathode with a discharged cathode of NaCl and Fe particles for the reversible reaction.

$$2Na + FeCl_2 = 2NaCl + Fe \quad (11)$$

The sodium−sulfur battery has been commercialized in Japan, the zebra battery is being developed by the GE Corporation in the U.S. Since sodium is much less expensive than lithium and widely available, a sodium battery is to be preferred over a lithium battery, and the large capacity of these sodium cells has made them attractive for large-scale stationary energy storage. However, operation at higher temperatures of corrosive materials presents a challenge. On the other hand, solid electrolytes allow consideration of liquid and gaseous reactants; the solid oxide fuel cell (SOFC) uses a solid O^{2-} electrolyte and gaseous reactants, for example.

An all solid-state Li battery would, in principle, use an inorganic solid or a polymer Li^+ electrolyte. An inorganic solid Li^+ electrolyte has been used with thin solid electrodes in an all solid-state Li cell, but the volume changes in the electrodes on charge/discharge have not allowed retention of good electrode/electrolyte contact in a rechargeable storage battery. Polymer Li^+ electrolytes with a sufficiently large window and a Li^+ conductivity $\sigma_{Li} > 10^{-4}$ S cm^{-1} that retains a good contact with solid electrodes have yet to be demonstrated. On the other hand, a solid Li^+ electrolyte membrane separating different liquid electrolytes contacting the anode and cathode would offer the possibility, if it blocked Li^+ dendrites, of a lithium anode and a liquid or gaseous cathode reactant. A lithium anode would maximize the cell voltage and anode capacity; an air or liquid flow-through cathode reactant would increase greatly the capacity of the cathode and therefore of the cell. However, a solid Li^+ electrolyte separator that blocks dendrites from a Li anode would need to have a major ceramic component, but a sufficiently thin ceramic membrane would be too fragile. A practical solid-electrolyte separator membrane would need: (a) a $\sigma_{Li} > 10^{-4}$ S cm^{-1}; (b) the capability to block Li dendrites without being reduced; (c) to be chemically stable in the liquid electrolytes; and (d) to be easily fabricated into a mechanically robust, flexible thin membrane. These requirements would appear to require a ceramic-polymer composite, a fruitful field of chemistry that has yet to be systematically explored. Electronically conducting polymers have been used to coat $LiFePO_4$ particles[41] and to connect carbon-coated $LiFePO_4$ to a current collector in the absence of added carbon and binder to the active material of the electrode.[43,44] For the electrolyte membrane, a polymer that is an electronic insulator with a $\sigma_{Li} > 10^{-4}$ S cm^{-1} is needed for the ceramic/polymer Li^+ electrolyte separator membrane. An example of a possible ceramic component that has a $\sigma_{Li} > 10^{-3}$ S cm^{-1} at room temperature and is stable on contact with elemental Li is $Li_{7-x}La_3Zr_{2-x}Ta_xO_{12}$, which has the $B_3C_2O_{12}$ framework of the garnet $A_3B_3C_2O_{12}$ structure.[45] Like the spinel $[B_2]O_4$ framework, the garnet framework contains an interstitial space consisting of tetrahedral A sites bridged by octahedral sites sharing faces with two A sites on opposite sides, Figure 8. Li^+ has a high 3D room temperature mobility in these frameworks. Moreover, coating the surface of the electrolyte particles with a hydrophobic skin, e.g., polydopamine, allows Li^+ transport while stabilizing the electrolyte particles in an aqueous electrolyte.

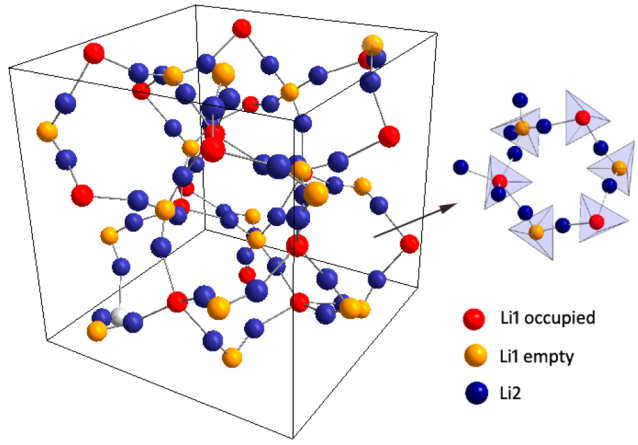

Figure 8. 3D connection of Li sites within the interstitial space of the garnet framework with 7.5 Li per formula unit. Loop structure and the separations of Li atoms are also displayed.

The air cathode offers a high capacity, but the reversible reaction:

$$4Li^+ + 4e^- + O_2 = 2Li_2O \quad (12)$$

requires inexpensive catalysts for the oxygen-reduction reaction (ORR) and the oxygen-evolution reaction (OER) at a high rate with a voltage difference $V_{ch} - V_{dis} \leq 0.3$ for storage efficiency, eq 2. Attempts to achieve this performance over a long cycle life in a nonaqueous electrolyte[46] with metallic Pt and Au catalysts have been disappointing, but a good performance may be achieved in an aqueous electrolyte with less-expensive oxide catalysts.[47,48] With only an aqueous electrolyte, as in the case of the Zn-air cell, the voltage is limited to ~1.5 V. With a solid Li^+ electrolyte separator of a nonaqueous electrolyte at a Li anode and an aqueous electrolyte at the air cathode, the voltage can be increased to ~3.5 V. Moreover, a flow-through redox couple in a liquid cathode that is separated from a Li anode by a solid Li^+ electrolyte membrane has also shown that an adequate voltage and capacity can be achieved at required power outputs for large, stationary storage of electric energy generated by wind, solar, or nuclear power.

The lithium−sulfur battery also provides a multielectron redox couple at the sulfur cathode and, therefore, a large increase in capacity,[49] especially in the form of a polysulfide redox couple in a flow-through liquid cathode.[50] But at 2 V vs Li, a practical sulfur cathode requires a Li anode and therefore either a solid Li^+ electrolyte separator or a liquid electrolyte with its LUMO shifted to an energy at least 0.5 eV above μ_A(Li).

A composite polymer gel containing a large volume fraction of an inorganic oxide and an organic liquid electrolyte immobilized in a polymer can give a flexible, thin membrane with a $\sigma_{Li} \approx 10^{-3}$ S cm^{-1}, but it needs yet to be tested as to whether it can block dendrites from a Li anode or soluble redox couples in a liquid

dx.doi.org/10.1021/ja3091438 | J. Am. Chem. Soc. 2013, 135, 1167−1176

cathode. Whether such an electrolyte, if coated with a surfactant, can permit use of an aqueous electrolyte for a Li/air battery needs to be explored. These are possible ways the chemist can design the needed breakthrough for low-cost Li-ion batteries that changes in our energy strategies call for.

SUMMARY

Dependence on the import of foreign oil makes the modern nation state vulnerable, which endangers international peace. The global impact of carbonaceous emissions from the internal combustion engine and coal-fired power plants has created a huge incentive to harvest and store electrical energy from wind and solar power. Electrical energy can be stored efficiently in a rechargeable battery, and the shift from an aqueous to the organic liquid-carbonate electrolyte in a LIB increased the energy density of a rechargeable battery sufficiently to enable battery-powered hand-held electronic devices and power tools; however these applications do not compete with devices powered by fossil fuels. The success of the LIB in powering the electronic revolution has revitalized interest in rechargeable batteries to displace the internal combustion engine where it must compete with the energy stored in a fossil fuel. This competition can only be successful in the near term where the battery stores electrical energy from the grid with off-peak power in a plug-in hybrid commuter vehicle. Another near-term target is storage of electrical energy generated by solar or wind power or for stabilizing the grid against variable demand for power. These latter applications appear to require increasing significantly the energy and power density over what is possible with a strategy that relies on a cathode composed of a solid host into which a singly charged cation is inserted reversibly over a finite solid−solution range.

Realization of this situation has led to consideration of either multiple-electron redox couples and/or multivalent working ions such as Mg^{2+} in place of Li^+. This shift of emphasis leads inevitably to the electrolyte, catalysts, and organic multiple-electron redox centers. We have emphasized here the potential of a Li^+ electrolyte membrane separating two different liquid electrolytes, a material that will require a composite of a polymer and an inorganic Li^+ electrolyte. We have not commented on efforts to introduce 3D current collectors that enable thicker electrodes and flow-through liquid cathodes, an effort that has particular relevance for electrochemical capacitors of higher energy density. We have also not commented on efforts to develop a Na-ion battery to eliminate vulnerability to sources of lithium and to lower material costs. This effort is more challenging because the larger Na^+ ion is adequately mobile only in framework oxides with a larger interstitial volume than is available in a close-packed oxide-ion array.

AUTHOR INFORMATION

Corresponding Author

jgoodenough@mail.utexas.edu

Notes

The authors declare no competing financial interest.

ACKNOWLEDGMENTS

Financial support of The Robert A. Welch Foundation grant no. F-1066 is gratefully acknowledged.

REFERENCES

(1) Yoshino, A.; Sanechika, K.; Nakajima, T. Japanese Patent 1989293, 1985.
(2) Zaghib, K.; Dontigny, M.; Guerfi, A.; Charest, P.; Rodrigues, I.; Mauger, A.; Julien, C. M. *J. Power Sources* **2011**, *196*, 3949.
(3) Kim, Y.; Park, K.-S.; Song, S. H.; Han, J.; Goodenough, J. B. *J. Electrochem. Soc.* **2009**, *156*, A703.
(4) Mitzushima, K.; Jones, P. C.; Wiseman, P. J.; Goodenough, J. B. *Mater. Res. Bull.* **1980**, *15*, 783.
(5) Gupta, R.; A. Manthiram, A. *J. Solid State Chem.* **1996**, *121*, 483.
(6) Kiehne, H. A. In *Battery technology handbook*; Expert Verlag: Renningen-Malsheim, Germany, 2003.
(7) Aurbach, D.; Talyosef, Y.; Markovsky, B.; Markevich, E.; Zinigrad, E.; Asraf, L.; Gnanaraj, J. S.; Kim, H. J. *Electrochim. Acta* **2004**, *50*, 247.
(8) Egashira, M.; Takahashi, H.; Okada, S.; Yamaki, J. *J. Power Sources* **2001**, *92*, 267.
(9) Fong, R.; van Sacken, U.; Dahn, J. R. *J. Electrochem. Soc.* **1990**, *137*, 2009.
(10) Zhang, X.; Kostecki, R.; Richardson, T. J.; Pugh, J. K.; Ross, P. N. *J. Electrochem. Soc.* **2001**, *148*, A1341.
(11) Steele, B. C. H. In *Fast Ion Transport in Solids*; van Gool, W., Ed.; North Holland Publishing: Amsterdam, 1973.
(12) Whittingham, M. S. *Science* **1976**, *192*, 1126.
(13) Peled, E. *J. Electrochem. Soc.* **1979**, *126*, 2047.
(14) Yamaki, J. In *Lithium Ion Batteries - Fundamentals and Performance*; Wakihara, M., Yamamoto, O., Ed.; Kodansha Ltd.: Tokyo, Japan, 1998; Chapter 4.
(15) Goodenough, J. B.; Wickham, D. G.; Croft, W. J. *J. Appl. Phys.* **1958**, *29*, 382.
(16) Yazami, R.; Touzain, Ph. *J. Power Sources* **1983**, *9*, 365.
(17) Zaghib, K.; Goodenough, J. B.; Mauger, A.; Julien, C. *J. Power Sources* **2009**, *194*, 1021.
(18) Whittingham, M. S. In *Intercalation Chemistry*; Whittingham, M. S., Jacobson, A. J., Ed.; Academic Press: New York, 1982; Chapter 1.
(19) Wu, E. J.; Tepesch, P. D.; Ceder, G. *Phys. Mag. B* **1998**, *77*, 1039.
(20) Delmas, C.; Saadoune, I. *Solid State Ionics* **1992**, *53−56*, 370.
(21) Guilmard, M.; Croguennec, L.; Delmas, C. *Chem. Mater.* **2003**, *15*, 4484.
(22) Choi, N. S.; Yew, K. H.; Lee, K. Y.; Sung, M.; Kim, H.; Kim, S. S. *J. Power Sources* **2006**, *161*, 1254.
(23) Kummer, J. T.; Weber, N. U.S. Patent 3,458,356, 1969.
(24) Goodenough, J. B.; Hong, H. Y.-P.; Kafalas, J. A. *Mater. Res. Bull.* **1976**, *11*, 203.
(25) Thackeray, M. M.; David, W. I. F.; Goodenough, J. B. *Mater. Res. Bull.* **1982**, *17*, 785.
(26) Thackeray, M. M.; David, W. I. F.; Bruce, P. G.; Goodenough, J. B. *Mater. Res. Bull.* **1983**, *18*, 461.
(27) Thackeray, M. M.; Johnson, P. J.; de Picciotto, L. A.; Bruce, P. G.; Goodenough, J. B. *Mater. Res. Bull.* **1984**, *19*, 179.
(28) Goodenough, J. B.; Loeb, A. L. *Phys. Rev.* **1955**, *98*, 391.
(29) Jahn, H. A.; Teller, E. *Proc. R. Soc. London, Ser. A* **1937**, *161*, 220.
(30) Liu, Z.; Yu, A.; Lee, J. Y. *J. Power Sources* **1999**, *81−82*, 416.
(31) Lu, Z.; MacNeil, D. D.; Dahn, J. R. *Electrochem. Solid State Lett.* **2001**, *4*, A191.
(32) Kim, J.-S.; Johnson, C. S.; Vaughey, J. T.; Thackeray, M. M.; Hackney, S. A.; Yoon, W.; Grey, C. P. *Chem. Mater.* **2004**, *16*, 1996.
(33) Zhong, Q.; Bonakdarpour, A.; Zhang, M.; Gao, Y.; Dahn, J. R. *J. Electrochem. Soc.* **1997**, *144*, 205.
(34) Kim, J.-H.; Yoon, C. S.; Myung, S.-T.; Prakash, J.; Sun, Y.-K. *Electrochem. Solid-State Lett.* **2004**, *7*, A216.
(35) Liu, J.; Manthiram, A. *J. Phys. Chem. C* **2009**, *113*, 15073.
(36) Arun Kumar, T. A.; Manthiram, A. *Electrochim. Acta* **2005**, *50*, 5568.
(37) Padhi, A. K.; Nanjundaswamy, K. S.; Masquelier, C.; Okada, S.; Goodenough, J. B. *J. Electrochem. Soc.* **1997**, *144*, 1609.
(38) Padhi, A. K.; Nanjundaswamy, K. S.; Masquelier, C.; Goodenough, J. B. *J. Electrochem. Soc.* **1997**, *144*, 2581.
(39) Padhi, A. K.; Nanjundaswamy, K. S.; Goodenough, J. B. *J. Electrochem. Soc.* **1997**, *144*, 1188.
(40) Park, K.-S.; Xiao, P.; Kim, S. Y.; Dylla, A.; Choi, Y. M.; Henkelman, G.; Stevenson, K. J.; Goodenough, J. B. *Chem. Mater.* **2012**, *24*, 3212.
(41) Lepage, D.; Michot, C.; Liang, G.; Gauthier, M.; Schougaard, S. B. *Angew. Chem., Int. Ed.* **2011**, *50*, 6884.

(42) Coetzer, J. *J. Power Sources* **1986**, *18*, 377.
(43) Park, K.-S.; Schougaard, S. B.; Goodenough, J. B. *Adv. Mater.* **2007**, *19*, 848.
(44) Huang, Y. H.; Park, K.-S.; Goodenough, J. B. *J. Electrochem. Soc.* **2006**, *153*, A2282.
(45) Li, Y.; Han, J. T.; Wang, C. A.; Xie, H.; Goodenough, J. B. *J. Mater. Chem.* **2012**, *22*, 15357.
(46) Christensen, J.; Albertus, P.; Sanchez-Carrera, R. S.; Lohmann, T.; Kozinsky, B.; Liedtke, R.; Ahmed, J.; Kojic, A. *J. Electrochem. Soc.* **2012**, *159*, R1.
(47) Suntivich, J.; May, K. J.; Gasteiger, H. A.; Goodenough, J. B.; Shao-Horn, Y. *Science* **2011**, *334*, 1383.
(48) Suntivich, J.; Gasteiger, H. A.; Yabuuchi, N.; Nakanishi, H.; Goodenough, J. B.; Shao-Horn, Y. *Nat. Chem.* **2011**, *3*, 546.
(49) Rauh, R. D.; Abraham, K. M.; Pearson, G. F.; Surprenant, J. K.; Brummer, S. B. *J. Electrochem. Soc.* **1979**, *126*, 523.
(50) Manthiram, A.; Fu, Y.; Su, Y. S. *Acc. Chem. Res.* **2012**, DOI: 10.1021/ar300179v.